Hydrogenation of biobased aldehydes to mono-alcohols using bimetallic catalysts

Article

Hydrogenation of biobased aldehydes to mono-alcohols using bimetallic catalysts

Giuseppe Bagnato, Michela Signoretto, Cristina Pizzolitto, Federica Menegazzo, Xiaoying Xi, Gert H. ten Brink, Bart J. Kooi, Hero Jan Heeres, and Aimaro Sanna

ACS Sustainable Chem. Eng., **Just Accepted Manuscript** • DOI: 10.1021/acssuschemeng.0c02623 • Publication Date (Web): 20 Jul 2020

Hydrogenation of biobased aldehydes to mono-alcohols using bimetallic catalysts

Giuseppe Bagnato[†, ‡], Michela Signoretto[§], Cristina Pizzolitto[§], Federica Menegazzo[§], Xiaoying Xi[‡], Gert H. ten Brink[‡], Bart J. Kooi[‡], Hero Jan Heeres[‡], Aimaro Sanna[, †]*

[†]Advanced Biofuels Lab, Institute of Mechanical, Process and Energy Engineering, School of Engineering & Physical Sciences, Heriot-Watt University, Edinburgh EH14 4AS, UK.

[§]CATMAT Lab, Department of Molecular Sciences and Nanosystems, Ca' Foscari University Venice and INSTM-RU Ve, Via Torino 155, 30172 Venezia Mestre, IT.

[‡]Department of Chemical Engineering, Engineering and Technology Institute Groningen, University of Groningen, 9747 AG Groningen, NL.

ABSTRACT A series of mono- and bi-metallic metal catalysts (Pd, Cu, Fe, PdCu, PdFe) supported on ZrO_2 (6-8 μm) were synthesised and tested for the hydrogenation of bio-oil model compounds (furfural, vanillin, glucose) under 50 bar H_2 at 100°C. The catalysts were fully characterised and their properties related to their catalytic activity.

The bi-metallic PdFe and PdCu displayed enhanced catalytic performance compared to the monometallic catalysts for aldehyde hydrogenation (furfural, vanillin, glucose). For the best catalyst, 98% vanillin alcohol (VA) and 65.5% furfuryl alcohol (FA) conversion was obtained

for 80 min batch-time. PdFe showed high selectivity towards sorbitol (74%) from glucose, though at low conversion (20%).

Overall, we have demonstrated that bimetallic Fe and Cu based catalysts promoted by Pd show significantly better performance for the partial hydrogenation of bio-oil model compounds than the corresponding monometallic ones. The better performance of the Pd doped Fe/Cu catalysts is linked to the presence of smaller and better dispersed Pd nanoparticles (STEM) and their lower acidity (~90 μmol/g cat) than corresponding monometallic ones (~ 167 μmol/g cat).

KEYWORDS: *Hydrogenation, furfural, vanillin, glucose, bimetallic catalysts*

INTRODUCTION

Fast pyrolysis of biomass to bio-oil is an attractive technology due to its low environmental impact, scalability and cost-competitiveness[1-2]. The current manufacturing costs are estimated at about $300/t [3], which is higher than for typical fossil based energy carriers. Moreover, bio-oil aging and phase stability are other main limitations.

The selective hydrogenation of the carbonyl bond of (unsaturated) aldehydes to form the corresponding (unsaturated) alcohols has received high attention because the products are widely used in industry [4-6]. Moreover, the hydrogenation of aldehydes such as furfural and phenolics such as vanillin can consistently improve the stability of the bio-oil and its aging, due to the reduction of Novolak resins formation[7]. Furfural is a compound derived from hemicellulose and its production is estimated at about around 300 kton per annum. Possible products from reactions of furfural with hydrogen in the presence of metal catalysts are shown in Figure 1 a)[8]. Partial hydrogenation leads to furfuryl alcohol (FA), which is an important chemical intermediate for the production of chemical products, such as vitamin C, lysine, plasticisers, dispersing agents and lubricants[9-10]. Vanillin (VL) can also be partially

hydrogenated to vanillin alcohol (Figure 1 b)), which finds application in foods, beverages, pharmaceuticals industries, and renewable polymers. VL current production is around 12-14 kton per year[11]. Moreover, lignocellulosic biomass derived bio-oils contain a large amount of sugar derived compounds such as glucose, levoglucosan and cellobiose. Glucose represents a platform for the production of numerous chemicals (e.g. sorbitol) by hydrogenation reaction (Figure 1 c).

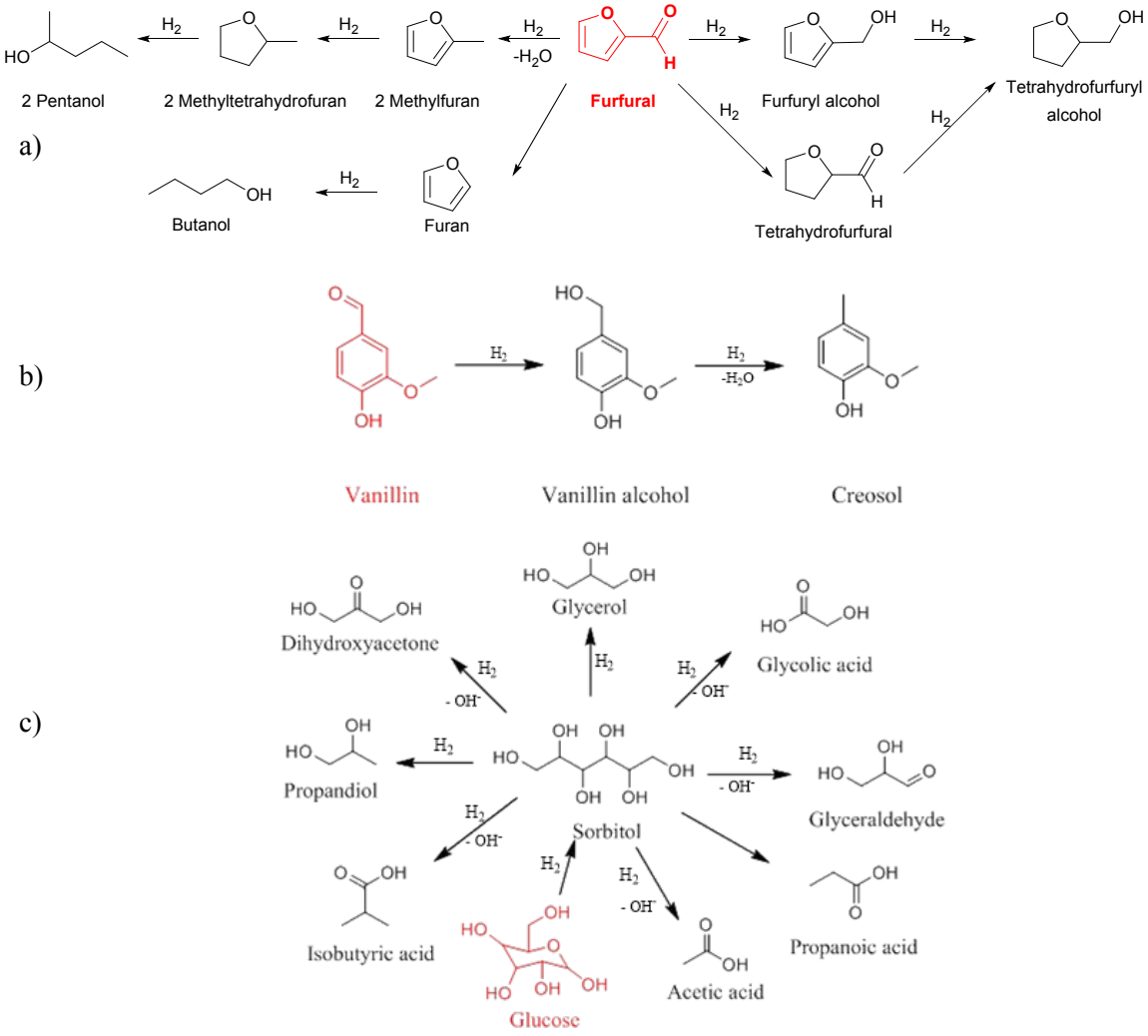

Figure 1. Catalytic hydrogenation products for a) Furfural, b) Vanillin and c) Glucose.

Numerous heterogeneous catalysts have been reported for the selective hydrogenation of furfural, vanillin and glucose. Typically, noble metals such as platinum, palladium, rhodium and ruthenium are used, which are expensive. Recent trends in nano-catalysis have shown that

supported bimetallic catalysts show often improved performance compared to their monometallic analogues due to synergistic effects (electronic, geometric, other interfacial effects) [12].

When considering furfural hydrogenation to alcohols, the objective of the current study, Cu based catalysts have shown good performance [13]. Preferential aldehyde reduction is observed, without competitive hydrogenation of the C=C bonds. Improved bimetallic catalysts, notably with Cr (VI), have been reported, though the use of Cr(VI) is not considered green due to its carcinogenic properties. Recently, Pt, Pd, Ru, Re and Ni have been shown to be good alternatives to Cr [14-17]. For instance, Fulajtárova *et al.* (2015) showed that furfural was quantitatively hydrogenated to FA with a selectivity of 86% using a bimetallic Cu (5%) - Pd (1%) catalyst supported on MgO (80 bar H_2, 130°C, 480 min). Du *et al.* reported studies on the hydrogenation of furfural using bimetallic Cu (2.66%) - Pd (0.25%) catalysts supported on carbon in 1,4-dioxane (170°C, 3 h) using formic acid as the H-donor and obtained high selectivity to FA (> 96%) at 100% furfural conversion [15].

Bimetallic Ni based catalysts have also been explored. Sitthisa et al. (2011) showed that the addition of Fe to Ni suppresses the decarbonylation activity of Ni[18-19], which is a major issue. Shi et al (2019) reported a 74% selectivity to FA at ~97% conversion using a $Fe_{50}Ni_{50}/SiO_2$ catalyst at 150 °C, 20 bar H_2 (2 h) and isopropanol as the solvent[20]. These studies clearly indicate that supported Fe and Cu based catalyst promoted with noble metals are of high interest for the hydrogenation of furfural to FA.

Hydrogenation of vanillin is typically performed using monometallic noble-metals (Ru and Pd) [21]. A number of Pd nanoparticles (NPs) on different supports[22-24] have also been reported for vanillin hydrogenation to VA. It was found that their application is limited due to catalyst stability issues associated with leaching of metal nanoparticles. The use of bimetallic Cu-Pd catalysts has been reported recently[21]. CuPd catalysts on N-rich porous organic polymers were

shown to be highly efficient catalyts compared to their monometallic counterparts, providing 99.3% conversion of vanillin with a selectivity of 93.6% for the hydrogenolysis product 2-methoxy-4-methylphenol at 140 °C, 10 bar H_2 in isopropanol [21].

When considering the selective hydrogenation of the aldehyde moiety in glucose to sorbitol, a number of monometallic catalysts have been developed. Commercially, sorbitol is obtained by using Raney Ni. Ru/C has shown to be a very attractive alternative achieving yields close to 100%, however it is expensive and prone to coking and sulphur deactivation [25]. The addition of Cu NPs to Ru/C resulted in a 50% enhanced catalytic activity in glucose hydrogenation (100°C, 80 bar H_2, 3 h, 30 mL of 40% glucose in water, 500 mg catalyst) [26], while the addition of Fe to Pt enhanced the catalyst activity for the hydrogenation of aldehydes, with TOF increasing from 7.8 min^{-1} (Pt), to 480 min^{-1} (PtFe), which was ascribed to stabilisation of adsorbed reactive intermediates on the Pt-Fe interface through bonding with C=O groups[27].

The above literature indicates that Fe and Cu based catalysts, which are 3 and 2 order of magnitude cheaper than Pd, are not very effective for aldehyde hydrogenation. However, little is known about the use of bimetallic Fe catalysts promoted with Pd for the hydrogenation of furfural and also only one paper is available for a Cu catalyst promoted by Pd for the hydrogenation of vanillin, while none are available for CuPd for glucose and FePd for vanillin and glucose hydrogenation.

We here report an experimental investigation on the use of novel bimetallic catalysts comprising of a cheap metal (Fe, Cu) combined with a noble metal, as Pd due to its high activity at mild conditions, for the aqueous phase hydrogenation of an aldehyde (furfural, vanillin and glucose), with the aim to obtain alcohols (FA, VA and sorbitol). Performance of the bimetallic catalysts was compared to that of the monometallic analogues. ZrO_2 was selected as the support as i) it is known to be stable in aqueous media at elevated temperatures[13], and ii) is it less prone to deactivation (compared to TiO_2 and C) [28 29]. The catalysts were characterised in detail and

performance was tested in a batch set-up using aqueous solutions of the three model components

EXPERIMENTAL DETAILS

Chemicals

Furfural 99% (CAS Num. 98-01-1), furfuryl alcohol 98% (CAS Num. 98-00-0), vanillin (CAS Num.121-33-5), vanillin alcohol ≥ 98% (CAS Num. 498-00-0), D-glucose ≥ 99.5% (CAS Num. 50-99-7) sorbitol ≥ 98% (CAS Num. 50-70-4) were purchased from Sigma-Aldrich. Tetrahydrofuran for HPLC (THF, CAS Num. 109-99-9), di-*n*-butyl ether >99% (DBE, CAS Num. 142-96-1) Fisher Scientific.

Catalysts synthesis

Support synthesis: $Zr(OH)_4$ was prepared by the dropwise addition of required amount of aqueous 1M solution of $ZrOCl_2{\cdot}8H_2O$ (Aldrich, 99.5%) to water (100 ml). During addition, the pH was kept constant at 8.5 by the dropwise addition of an aqueous solution of ammonia (5 M). After addition, the suspension was aged 20 hours at 90 °C. The resulting $Zr(OH)_4$ was isolated by filtration , washed free from chloride ($AgNO_3$ test), dried in an oven at 110 °C for 15 h and subsequently calcined in flowing air (30 mL/min) at 500 °C for 3 h to obtain the ZrO_2 support[30]. Catalyst synthesis: an incipient wetness (co) impregnation method was applied to prepare the catalysts, due to its suitability for large scale applications. The proper amount of an aqueous solution of the metal precursor ($PdCl_2$, $FeN_3O_9{\cdot}9H_2O$ or $Cu(NO_3)_2{\cdot}3H_2O$) were simultaneously added to the ZrO_2 support to obtain the desired metal content on the support (5 wt% for Cu and Fe, 1 wt % for Pd). The catalysts were dried in an oven at 110 °C for 15 h and finally calcined in flowing air (30 mL/min) at 500 °C for 3 h.

Catalysts characterisation

A detailed description of the methods used for the catalysts' characterisation is reported in the supplementary material. The metal amount on the catalyst was determined by Atomic Absorption Spectroscopy (AAS) using a Perkin-Elmer Analyst 100. TEM analysis were carried out using a CM12 microscope (Philips), operating at 120 keV. High-angle annular dark-field scanning transmission electron microscopy (HAADF-STEM) images were obtained with a ThemisZ microscope (Thermo Fischer Scientific). Energy dispersive X-ray spectroscopy (EDX mapping) results were achieved with a Dual X EDX system (Bruker). TPR measurements were carried out using a home-made device. Nitrogen physisorption analyses were performed using a Tristal II Plus Micromeritics analyser. TPO was applied to characterise the carbon species on spent catalysts using a home-made device. The surface acidity of the catalysts was determined using NH_3-TPD measurements on an AutoChem II system (Micromeritic, USA) and the total acidity quantified. CO_2-TPD was run using a TA Q500. XPS analysis were carried out using a Scienta XPS with Al Kα (1486.6 eV) monochromatized ($\Delta\varepsilon < 300$ meV) source. O_2/H_2 pulse chemisorption measurements[31] were performed in the same lab-made equipment used for TPR, while a Thermo Scientific Nicolet 1S5 model with a 1D7 ATR attachment was used for the Fourier-transform infrared spectroscopy (FTIR).

Catalysts testing protocols

The hydrogenation reactions were carried out in a batch reactor (stainless-steel, 50 mL, Amar Equipments LTD, model no. 1233). The reactor was equipped with a heating jacket to allow operation at constant temperature. The reactor was loaded with 200 mg of catalyst and 30 mL of an aqueous solution of the model component (0.519, 0.204 and 1.07 mol/L for furfural, vanillin and glucose, respectively) and subsequently pressurised using H_2. The concentration of the model compounds resembled the real overall amount of the specific functional group into WBO from pinewood (BTG bio-oil). All reactions were carried out at 100 °C, 50 bar, and under continuous stirring (600 rpm). Before each experiment, the catalyst was activated overnight in

the presence of H_2 at 20 bar at 100 ºC (PdFe and Pd), 200 ºC (PdCu and Cu) or 300 ºC (Fe). The reduction temperatures were determined by TPR analysis. The overnight procedure was chosen in order to have a complete reduction of the active metals as suggested by previous authors[32]. The reduction of ferrous to metallic ions at 500 °C (as suggested by H_2-TPR) was not pursued due to possible interaction of the Fe^{2+} ions with the ZrO_2 support[33].

To evaluate the performance of the catalysts, the conversion, selectivity and TOF were calculated for the *i*- model compound using eq. 1 and 2.

$$Conversion_i = \frac{mole\ reacted}{initial\ mole}\Big|_i 100 = [\%] \quad (1)$$

$$Selectivity_j = \frac{mole\ produced_j}{mole\ reacted_i}\left|\frac{\nu_i}{\nu_j}\right| 100 = [\%] \quad (2)$$

$$TOF = \frac{mole_i|_{t=0} - mole_i|_{t=reaction\ time}}{total\ mole\ of\ metal\ on\ catalyst\ \cdot\ reaction\ time} = [h^{-1}] \quad (3)$$

Where, ν_i and ν_j represent the stoichiometric coefficients of i- and j- compounds, and the total moles of metal on the catalyst are the moles of Cu, Pd and Fe for the monometallic catalysts and the sum of the moles of metals for the bimetallic ones. Conversion levels below 20 % of the maximum equilibrium conversion were employed to calculate furfural and glucose TOFs to minimise possible issues associated with excess of catalyst, undesired catalyst deactivation, and surface coverage. However, this was not possible for vanillin, since the initial conversion was already higher than 20% of the equilibrium conversion, so that the TOFs in this case were estimated by curves fitting at conversion <20%.

To evaluate if the system was operating free of mass transport limitations, the external (η_{ex}) and internal (η_{in}) mass transport effectiveness factors were estimated (See Supplementary material) by the Damköhler number ($D_{II,b}$) and observed Thiele modulus, respectively.

Product characterisation

The glucose concentration was determined by HPLC using a Hewlett Packard 1050 system equipped with a Bio-Rad Organic Acid column (Aminex HPX-87H), and a Waters 410

differential refractometer. Aqueous sulphuric acid (5 mmol/L) was used as the mobile phase (0.55 mL/min). The column was maintained at 60º C. Furfural and vanillin hydrogenation products were analysed by a Shimadzu GC-2010A gas chromatograph equipped with a FID detector using a CPWAX 57-CB column (25 m × 0.2 mm × 0.2μm).

RESULTS AND DISCUSSION

Catalysts characterisation

The textural properties of the catalysts and the actual metal contents are reported in Table 1 and are discussed in the supplementary material.

The XRD patterns of the catalysts are provided in Figure S3 (supporting information). The reflections were identified by using the Crystallography Open Database [34]. In all the samples, reflections of the zirconia support were clearly detected and showed that presence of mostly monoclinic crystallites. Application of the Sherrer' equation for major ZrO_2 reflections revealed a particle size range of about 6-8.4 nm (Table 1), which is slightly smaller than found using TEM. The Fe, Cu and Pd were mainly present in the oxidic form.

Two of the catalysts (Pd/ZrO_2 and $PdCu/ZrO_2$) were characterised in more detail by STEM-EDX and the results are given in Figure 2 and Figure 3. Figure 2 shows that the Pd nanoparticles in Pd/ZrO_2 have a nanoparticle size of about 5 nm. In contrast, nanoparticles of Pd and Cu were not clearly visible in the bimetallic $PdCu/ZrO_2$ catalyst. EDX mapping shows that Pd and Cu are well dispersed. The dispersion of Cu on zirconia surface derives from the intimate contact between Cu and ZrO_2, caused by the oxygen vacancies in latter that play key roles in determining the dispersion of the active metal component[35]. The adsorption of Cu at ZrO_2 surface hydroxyl sites upon deposition is favoured at lower copper surface densities (as used in this work) and facilitates higher levels of Cu dispersion[36]. Moreover, previous work shows that the addition of Cu into Pd supported on ZrO_2 with monoclinic crystalline structure result in Cu

and Pd particles in intimate contact and highly dispersed in the support [37]. This is consistent with the STEM-EDX results showing good Pd dispersion. These distinct differences are expected to have impacts on catalyst performance (*vide infra*).

208 **Table 1.** Relevant catalyst properties.

	Metal content[a] (%)			Specific surface area[b] (m^2/g)	Pore volume[c] (cm^3/g)	Mean support pore diameter[c] (nm)	Mean support particles diameter[e] (nm)	H_2 uptake, µmol/g	Weak acid sites [f,g] (µmol NH_3/g cat)	Strong acid sites [f,h] (µmol NH_3/g cat)	Total acidity (µmol NH_3/g cat)	Total basicity (µmol CO_2/g cat)
	Pd	Fe	Cu									
Pd/ZrO_2	1.11	-	-	66	0.27	19.9	7.3 ± 0.5	350	167	165	332	-
$PdFe/ZrO_2$	1.00	4.11	-	68	0.25	18.6	8.4 ± 0.6	98	91	78	169	190
$PdCu/ZrO_2$	1.05	-	4.68	60	0.26	18.3	6.1 ± 0.4	290	92	88	180	120
Fe/ZrO_2	-	5.05	-	64	0.24	18.8	7.4 ± 0.6	280	111	119	260	160
Cu/ZrO_2	-	-	4.28	61	0.25	18.4	8.0 ± 0.5	280	109	152	261	90
	[a] From Atomic Absorption Spectroscopy analyses, [b, c] From N_2 physisorption analyses, [d]BJH, [e] From Sherrer`s equation [f] by peak's deconvolution from data obtained by AutoChem II system (Figure S5), [g]Weak acid sites temperature range 100-210 ºC, [h] Strong acid sites temperature range 210-400 ºC											

209

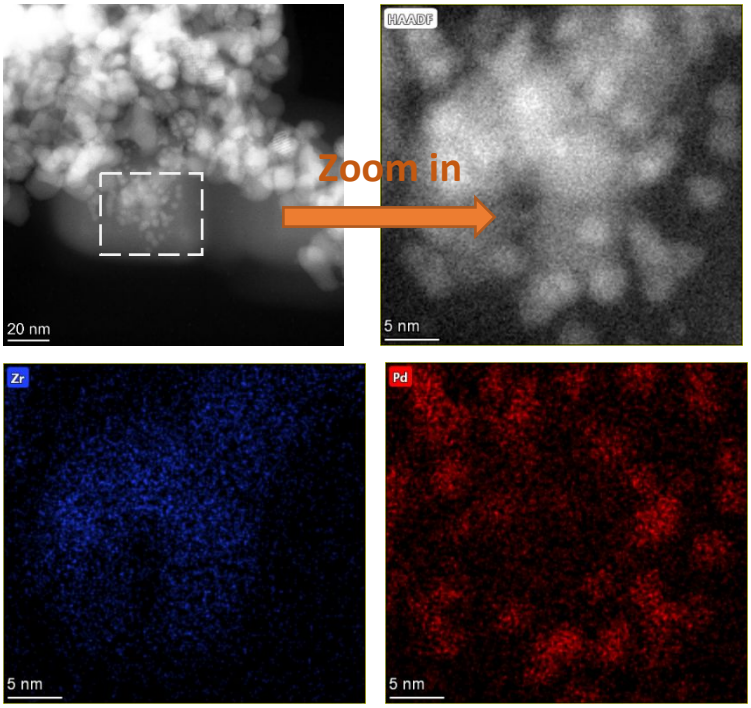

Figure 2. STEM- EDX image of the Pd/ZrO_2.

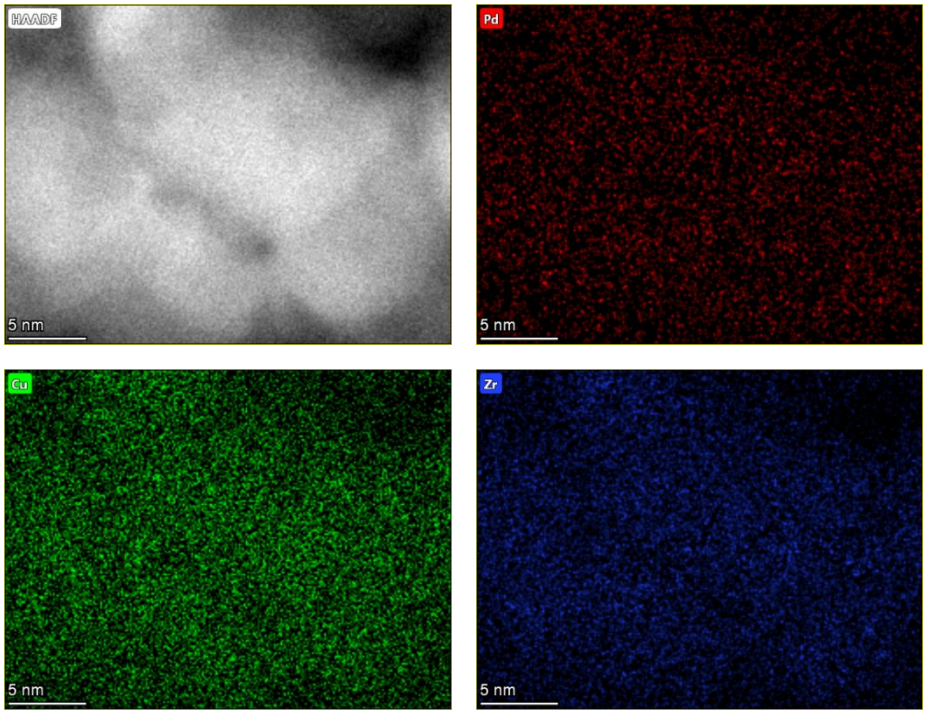

Figure 3. STEM- EDX image of the $PdCu/ZrO_2$.

H_2-TPR data for the different catalysts are provided in Table 1 and the supplementary information (Figure S4). The studied catalysts present similar H_2 uptake (~280-350 µmol/g), the only exception being $FePd/ZrO_2$ (98 µmol/g). For the monometallic Pd/ZrO_2 catalyst, only

one clear peak is observed at around 100 °C, which is attributed to Pd metal formation from the oxide phase [38-40]. Zr^{4+} reduction does not take place in the measured temperature range (max 700°C), in line with literature data [41]. The monometallic Cu/ZrO_2 catalyst shows two peaks, one at about 200 ºC assigned to the reduction of CuO to Cu_2O, and a broad peak between 250 and 400°C, assigned to the consecutive reduction of Cu_2O to Cu°. The presence of the two overlapping peaks can be attributed to the different CuO species that are differently interacting with the support[42-43]. The H_2-TPR spectrum of the bimetallic $CuPd/ZrO_2$ shows one clear band from Cu (~230°C) and a shoulder (~300°C) assigned to reduction of Cu_2O to Cu°. The peak from Cu reduction is shifted to higher temperatures compared to monometallic Cu/ZrO_2, indicating Cu-Pd interaction[15] . The Fe/ZrO_2 catalyst shows clear peaks at about 300, 400 and 520 °C, associated with several reduction steps ($Fe_2O_3 \rightarrow Fe_3O_4 \rightarrow Fe$) [44]. In the bimetallic Fe-Pd catalyst, the main reduction peaks of Fe_2O_3 are shifted to lower temperature, indicating a much stronger capability of $FePdZrO_2$ (compared to $FeZrO_2$) in adsorbing H_2 at low temperature.

Figure S5 shows the NH_3-TPD profiles of the catalysts studied in this work. For all the samples an overlap of weak (160-210 ºC) and strong acid peaks (240-340 °C) was observed. NH_3-TPD reveal that the bimetallic catalysts are less acidic than the monometallic ones (Table 1), with acidity similar to that of bare ZrO_2 (~160 μmol NH_3/g_{cat}) [45]. The monometallic Pd/ZrO_2 catalyst was the most acidic, with 332 μmol NH_3/g_{cat} desorbed, while $PdFe/ZrO_2$ was the least acidic (169 μmol NH_3/g cat). XPS spectra for the monometallic Fe/ZrO_2 catalyst (Figure S6) show two Fe 2p binding energy (BE) bands from Fe_3O_4 (711 eV and 715 eV) and one for Fe_2O_3 (725 eV). In the bimetallic $FePd/ZrO_2$ catalyst, these bands shift to higher BE's, which suggest the presence of Fe-Pd interactions. XPS spectra for monometallic Cu/ZrO_2 (Figure S7) indicate the presence two peaks corresponding to Cu^0 (934.4 and 952 eV)[46]. For the bimetallic Cu based catalyst, the shake-up features of Cu $2p_{3/2}$ were very similar to those of the monometallic Cu

catalyst, but with lower binding energy, suggesting interaction between Cu and Pd, as found by the H_2-TPR analysis.

Furfural hydrogenation

The hydrogenation of furfural using the mono-and bimetallic catalysts was performed in a batch autoclave at 100 °C, 50 bar hydrogen and using water as the solvent. Mass-transfer resistances (external and internal diffusion limitations) were absent in presence of furfural, as both the internal and external effectiveness were ~1 (See Table S8). The concentration of furfural was 0.519 M and the substrate-catalyst ratio was set at 7.48 g/g. The catalyst performance data are given in Table 2 and Figure 4. Some experiments were performed in duplicate and the error in the conversion was shown to be about 7%. All catalysts gave close to quantitative selectivity to FA and neither ring hydrogenation nor decarbonylation, well known side reactions were observed. The highest furfural conversion was obtained with the bimetallic $PdCu/ZrO_2$ catalyst (~70% after 80 min), which is considerably higher than for the monometallic Cu/ZrO_2, A similar trends, i.e. the higher activity of the bimetallic PdFe catalyst compared the monometallic Fe one, was found for the Fe based catalysts.

A possible explanation is the better dispersion of the metals for the bimetallic catalysts compared to the monometallic ones, as was illustrated using STEM- EDX for the Pd and Cu based catalysts (Figure 2). To verify this, H_2 chemisorption for the Fe/ZrO_2 and $PdFe/ZrO_2$ was carried out. Chemisorption of O_2 (at 25°C) followed by H_2 titration (at 60°C) resulted in 0.17 mLH_2/g_{cat} and 2.03 mLH_2/g_{cat} chemisorbed respectively on Fe and $PdFe/ZrO_2$. These data well corroborate the STEM-EDX finding of a better metal dispersion for the bimetallic catalysts.

Table 2. Hydrogenation of furfural at 100 ºC, 50 bar, furfural 0.519 mol/L; 200 mg catalyst after 80 min.

Catalyst	Furfural conversion (%)	Furfuryl alcohol selectivity (%)	TOF (h^{-1})
5 wt.% Cu/ZrO_2	29.5	99	5.3
1/ 5 wt.% $PdCu/ZrO_2$	66.1	99	6.9
5 wt,% Fe/ZrO_2	26.1	99	6.5
1/ 5 wt.% $PdFe/ZrO_2$	54.7	99	2.1

1 wt.% Pd/ZrO_2	43.7	99	14

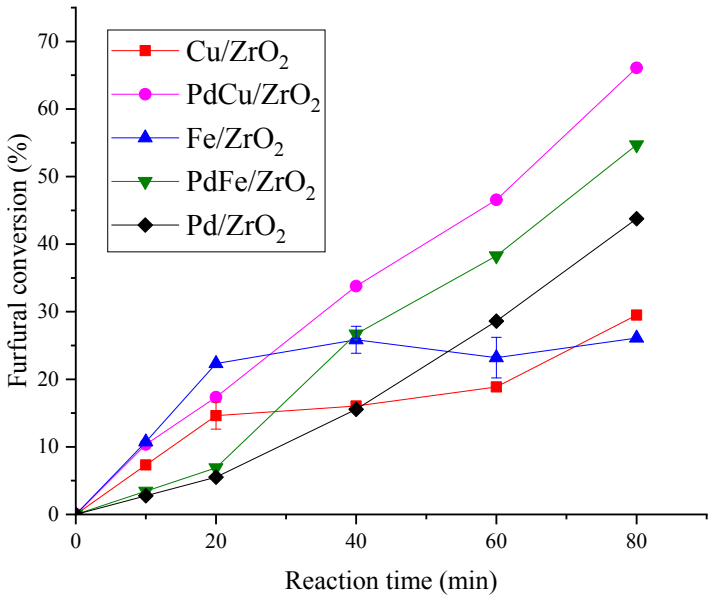

Figure 4. Hydrogenation of furfural at 100 ºC, 50 bar, 30 mL of furfural 0.519 mol/L, 200 mg of catalyst (furfural:catalyst wt ratio 7.48:1).

To establish a potential relation between the NPs size and the furfural conversion, the Pd and PdCu NPs were studied by scanning TEM (STEM)-EDX mapping (shown in Figure 2 and Figure 3). The Figures clearly indicate that while Pd/ZrO_2 presents distinct Pd nanoparticle with size of about 5 nm, there was a better dispersion of the Pd for $PdCu/ZrO_2$, with less agglomeration and smaller particle. Therefore, the better performance of the bimetallic PdCu is possibly related to the distinct difference in Pd NPs size that resulted in a better dispersion for the bimetallic PdCu.

Moreover, adding Pd to Cu can modify the structure and surface electronic properties of the Cu catalysts, which will affect the stability of intermediates and the adsorption capacity of Cu [47]. Since Cu has a half empty 4s band that can act as an electron donor or acceptor depending on the valence band of the different metal, while Pd has a fully filled 4d band, so that electrons will flow from the Pd 4d band into the Cu 4s band, stabilising the latter, where the furfural is

adsorbed via the η1 (O)-aldehyde binding with consequent hydrogenation of the C=O bond to form FA[48-49].

Considering the TOF, the best results were obtained using Pd/ZrO_2 (TOF=14 h^{-1}). Regarding selectivity, all the zirconia supported catalysts resulted in 99% selectivity towards FA. A recent work suggested that selectivity to FA is related to Cu content in PdCu/C, with 2.66-5.33% being the best content, while Pd content resulted not linked to FA selectivity [15]. Such correlation was not found in our work, since also Pd alone achieved 99% selectivity to FA, suggesting that the operating conditions are the drive for the high selectivity.

Vanillin hydrogenation

The hydrogenation of vanillin was studied under the same conditions used for furfural, but with a concentration of 0.204 M and a substrate-catalyst ratio of 4.65 g/g. Both internal and external diffusional resistances were not observed (Table S8). The catalysts performance is shown in Table 3 and Figure 5. Reproducibility was evaluated running two testes in triplicates with an average error of 2.2 %.

The catalysts show a 99% selectivity for partial hydrogenation to vanillin alcohol, and neither cresol (C-O bond cleavage) or guaiacol (C-C bond cleavage) were detected. The highest conversion of VL was obtained for $PdFe/ZrO_2$ (99.2%) and $PdCu/ZrO_2$ (98.2%) after 40 and 80 min, respectively, which was 2-fold (Cu/ZrO_2) and 2.5-folds (Fe/ZrO_2) higher than for the mono-metallic zirconia catalysts.

A synergic effect is exhibited by the bimetallic and in particular the PdFe catalyst. A previous study reported that Fe surface serves as the catalytic site for the activation of phenolic compounds and Pd stabilise Fe by its electronic interaction with Fe surface atoms [50].

Rezaei et al.(2016) reported that the oxophilicity of Fe metal cause repulsion to the phenolic ring, and in turn, a strong interaction with the carbonyl group, facilitating its selective hydrogenation to the corresponding alcohol[51]. Moreover, the H_2-chemisorption tests indicate

that the addition of Pd to Fe reduces the barrier to H_2 chemisorption of Fe. Furthermore, the addition of 1%Pd to 5%Cu (and possibly to Fe) is beneficial to the dispersion of the Pd nanoparticles as indicated by the H_2-chemisorption and TEM analyses, which can be linked to the enhanced hydrogenation activity of the bimetallic species (See Figure 5).

Table 3. Hydrogenation of vanillin at 100 ºC, 50 bar, 30 mL of vanillin 0.204 mol/L; 200 mg catalyst at 10 min.

* estimated at conversion <20%.

	Vanillin conversion (%)	Vanillin alcohol selectivity (%)	TOF* (h^{-1})
5 wt.% Cu/ZrO_2	51.4	99	22
1/ 5 wt.% $PdCu/ZrO_2$	98.2	99	41
5 wt. % Fe/ZrO_2	39.3	99	10
1/ 5 wt.% $PdFe/ZrO_2$	99.2	99	49
1 wt.% Pd/ZrO_2	71.6	99	250

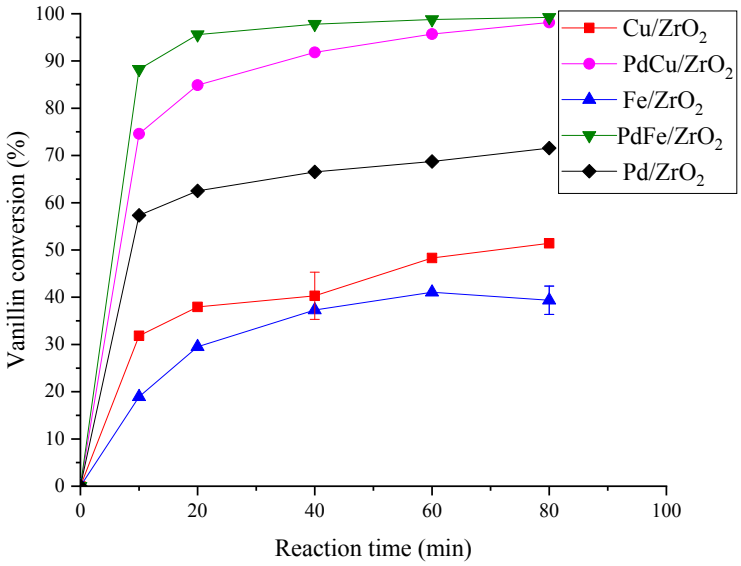

Figure 5. Hydrogenation of vanillin at 100 ºC, 50 bar, 30 mL of vanillin 0.204 mol/L; 200 mg catalyst (vanillin: catalyst wt ratio 4.65:1).

Previous works suggest that the partial hydrogenation of VL to VA is favoured in presence of basic sites[19,22,23]. All the ZrO_2 based catalysts possess basic sites as reported in Table 1, which can be linked to the high VA selectivity.

The comparison of the VL and FU conversion data indicates that the aldehyde group of vanillin is more reactive than the aldehyde group of furfural. This could be due to differences in interactions between either the substrate or product with the catalyst[24, 48].

Glucose hydrodeoxygenation

The hydrogenation of glucose with an initial concentration of 1.07 M and a substrate-catalyst ratio of 28.9 g/g was studied in water phase under the same conditions used for FU and VL. Under these conditions, internal and external diffusional resistances were not observed (See Table S8). The catalysts performances are reported in Table 4 and Figure 6. The conversion of glucose was relatively low (16-20%), possibly due to a high substrate- catalyst ratio used in comparison to previous works [52-54]. The TOF decreases in the following order: Pd/ZrO_2> $PdFe/ZrO_2$> Fe/ZrO_2> $PdCu/ZrO_2$> Cu/ZrO_2. Similarly to FU and VL, the highest glucose conversion (~20%) was achieved with the bimetallic catalysts, even if the conversion difference with the monometallic counterparts was less marked, which supports the finding that more dispersed Pd NPs (See Figures 2 and 3) in the bi-metallic species have a positive effect on the bio-substrate conversion.

Table 4. Hydrogenation of glucose at 100 ºC, 50 bar, 30 mL of glucose 1.07 mol/L; 200 mg catalyst (glucose: catalyst wt ratio 28.9:1) at 120 min.

	Glucose conversion (%)	Sorbitol selectivity (%)	TOF (h^{-1})
5 wt.% Cu/ZrO_2	18	34	$0.7 \cdot 10^{-2}$
1/ 5 wt.% $PdCu/ZrO_2$	20	52	$0.6 \cdot 10^{-2}$
5 wt. % Fe/ZrO_2	16	49	$0.6 \cdot 10^{-2}$
1/ 5 wt.% $PdFe/ZrO_2$	19	74	$0.6 \cdot 10^{-2}$
1 wt.% Pd/ZrO_2	18	58	$1.6 \cdot 10^{-2}$

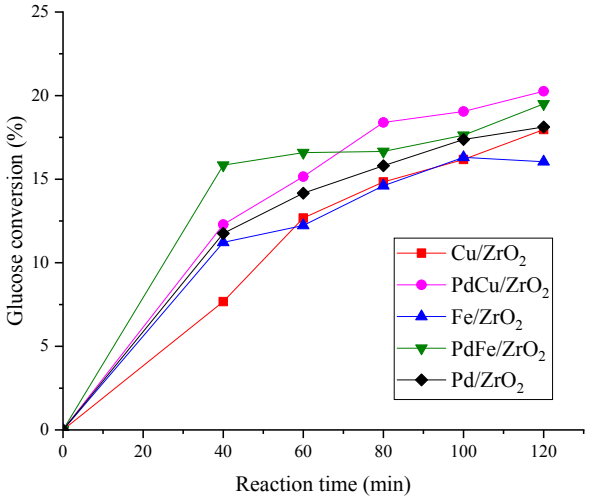

Figure 6. Hydrogenation of glucose at 100 ºC, 50 bar, 30 mL of glucose solution (1.07 mol/L); 200 mg catalyst (glucose: catalyst wt. ratio 28.9:1).

Contrary to FU and VL, the hydrogenation of glucose led to several products Figure 7) denoting the co-existence of multiple reactions under the studied conditions. The aldehyde group of glucose was hydrogenated to produce sorbitol, achieving a selectivity around 74% for $PdFe/ZrO_2$, while the lowest value (about 34%) was detected for the Cu containing catalysts. The catalyst selectivity for sorbitol decreased in the order: $PdFe/ZrO_2 > Pd/ZrO_2 > Fe/ZrO_2 > PdCu/ZrO_2 > Cu/ZrO_2$ suggesting that the dispersion of the Pd NPs in not linked to the product's selectivity. The different products distribution could be linked to the catalysts acidity[49]. Figure 8 shows the relation between the acidity of the catalysts and the selectivity towards sorbitol. As can be seen, excluding Pd, there is a clear trend, where the least acid catalyst (PdFe) resulted in the highest selectivity to sorbitol. Cu/ZrO_2 and in less extent $CuPd/ZrO_2$ favour the further hydrogenation or retro-aldol condensation of sorbitol to form glycerol and the hydrogenolysis to EG, PG etc and this explains its low selectivity towards sorbitol[54].

Zhang et al. (2016) obtained a 60 and 75% selectivity to sorbitol respectively at 40 and 60 bar at 140°C using 1.5% Pt-SBA-15 (calculated at 5% glucose conversion) [55]. In the same study, it was shown that the catalyst activity increased 3 folds when the temperature was increased

from 100 to 140 °C. This latter data can be used to compare the conversion obtained in our work, since similar metal loadings and H_2 pressure were used. Despite Ru and Pt are typically employed for the hydrogenation of glucose [55], here we show that Fe promoted by Pd has a good selectivity towards sorbitol.

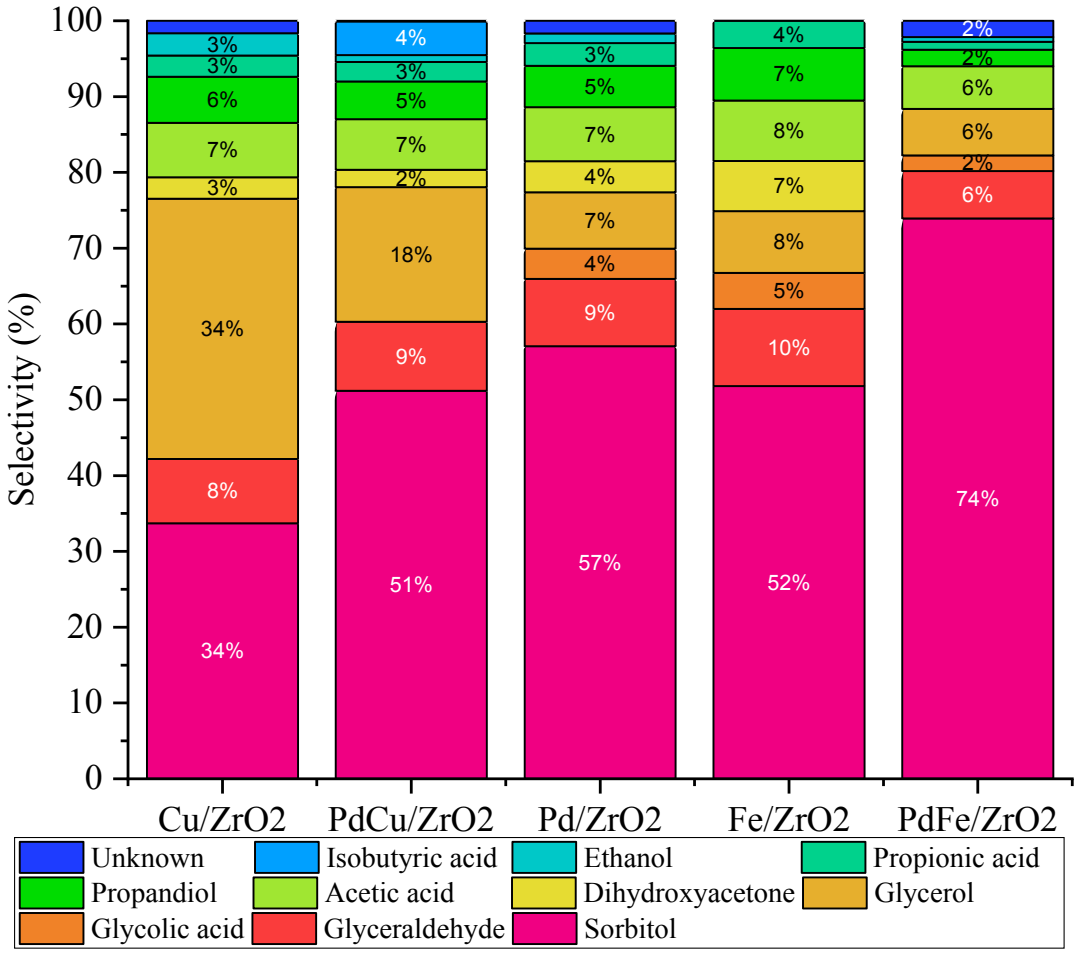

Figure 7. Selectivity of glucose hydrogenation at 100 ºC, 50 bar, after 120 min.

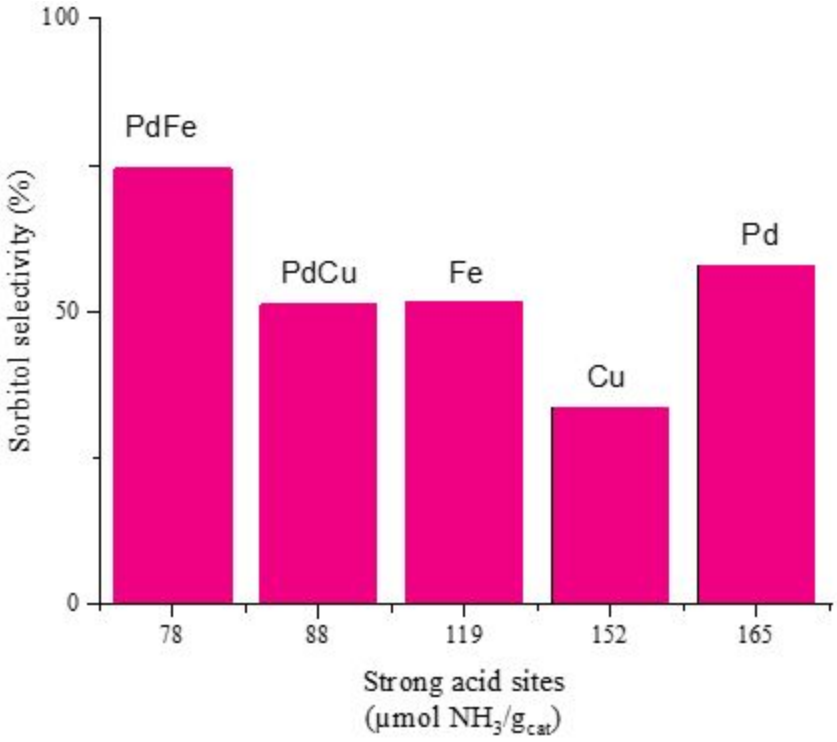

Figure 8. Sorbitol selectivity vs catalysts acidity at 40 min for hydrogenation of glucose at 100 ºC, 50 bar, 30 mL of glucose 1.07 mol/L; 200 mg catalyst (glucose: catalyst wt. ratio 28.9:1).

Catalysts deactivation study

Since the conversion versus batch time profiles for the reactants (see Figure 4) showed sign of deactivation for the mono-metallic catalysts, TPO was carried out to evaluate the presence of organic deposits on the catalysts' surface. Figure 9a and Table S7 indicate that poisoning by organic species (in terms of mg O_2 consumed/g catalyst) occurred during the reaction and increased in the following order for furfural: $PdFeZrO_2$ < $FeZrO_2$ < $PdZrO_2$ < $CuZrO_2$ < $PdCuZrO_2$. The TPO analyses of the spent catalysts from the vanillin hydrogenation instead suggest deposition of organics on the catalyst surface, mainly for the bimetallic catalysts, which are the most active (Figure 9b). Finally, the TPO analysis of spent catalysts from glucose hydrogenation (**Error! Reference source not found.**c) shows low oxygen consumption due to the low activity of the catalysts in hydrogenating glucose. The peak between 200 and 400 °C can be ascribed to coke, while the peak at about 180 °C, which is present in the $PdFe/ZrO_2$ and $PdCu/ZrO_2$, can be assigned to unreacted glucose.

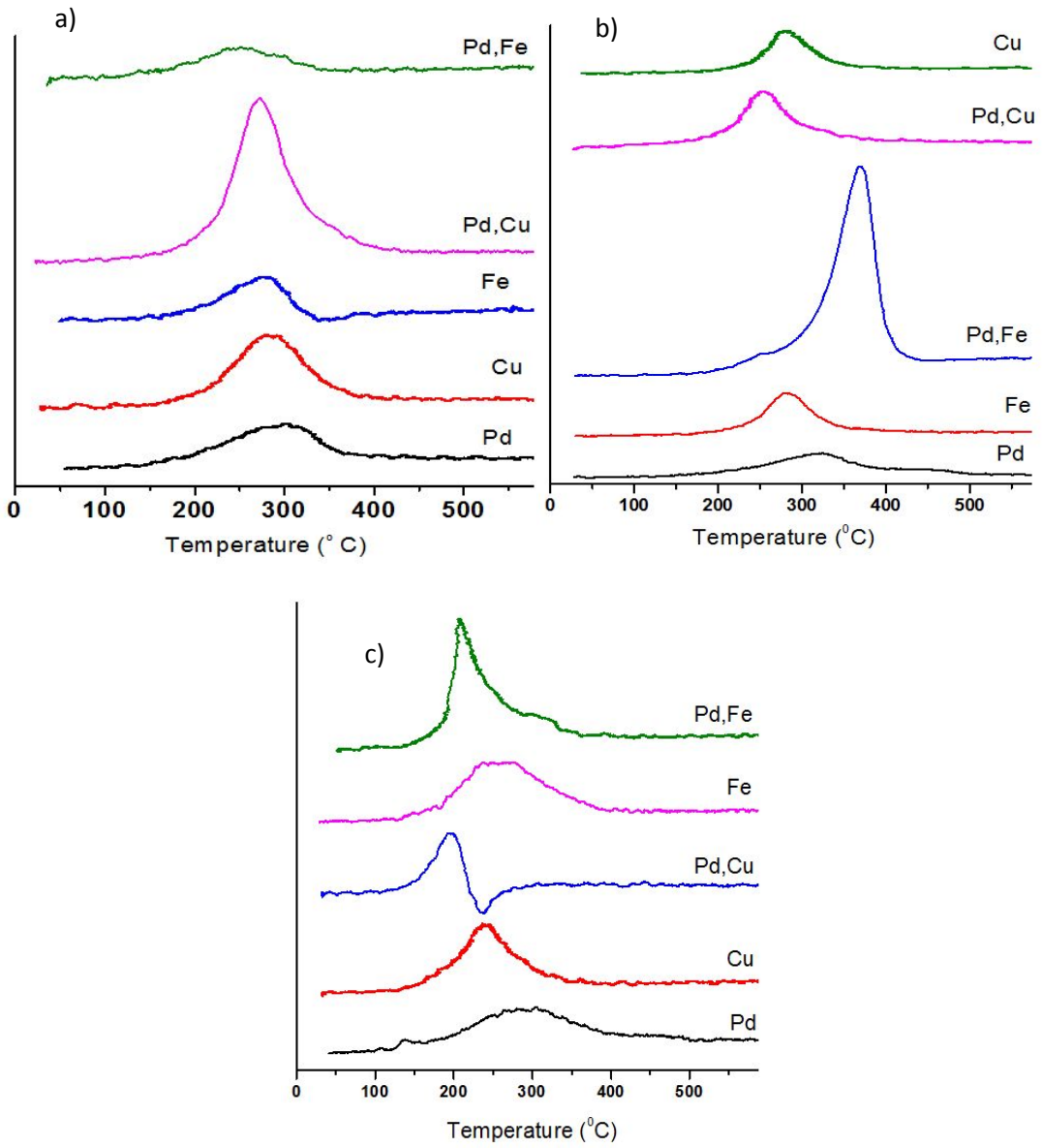

Figure 9.TPO analyses of spent catalysts after (a) furfural; (b) vanillin; (c) glucose hydrogenation reactions

EA of bare and spent catalysts (from furfural tests) were also carried out for coke quantification. Table 5 shows that $PdFe/ZrO_2$ had the least coke on surface, while $PdCu/ZrO_2$ resulted in the highest coke yield, in agreement with the TPO analysis. Coke deposition does not seem to be linked to the catalysts' deactivation, possibly due to the fact that coke formed at low temperature is less poisonous than more condensed coke generated at high temperature[56].

Table 5. EA of spent catalysts.

Spent catalyst	Wt%		
	C	H	H/C ratio
Pd/ZrO_2	2.01	0.14	0.07
Cu/ZrO_2	3.52	0.19	0.05
Fe/ZrO_2	2.94	0.14	0.05
$PdCu/ZrO_2$	4.54	0.29	0.06
$PdFe/ZrO_2$	1.94	0.13	0.07

To elucidate if the found organic deposits were made of coke or resulted from the deposition of unreacted furfural, FTIR of the spent catalysts (Figure S8) were performed. The broad peak between 3000 and 3400 cm^{-1} and 1530-1630 cm^{-1} are assigned respectively to weak C-H and C=C stretching vibration of aromatic groups [57]. The absence of strong transmittance bands in the range 1000-1300 cm^{-1}, which represent the C-O-C bending vibration indicates the absence of unconverted furfural or presence of produced furfyryl alcohol[57]. Presence of peaks at ~1400 cm^{-1} and the narrow bands caused by C-H out-of-plane bending mode in the range 650-900 cm^{-1} can be also associated to PAH molecules [58]. The H/C ratio (Table 5) of the coke on the catalysts surface somehow matches those of 2-ring PAH. Instead, H-depleted species that are typically formed at higher temperature seem to be absent on the catalysts surface [57], as confirmed by presence of H in the EA.

However, if the TPO data are compared to the conversion ones (Figure 4), deactivation by coking can be excluded, since Fe/ZrO_2 and Cu/ZrO_2 do not present the highest organic deposits, which instead seem to be proportional to the catalysts' activity. This also suggests that other causes such as metal sintering or leaching could be linked to the mono-metallic deactivation. To elucidate the presence of metal leaching and sintering, AAS and XRD analyses of the spent catalysts were carried out. The AAS indicates that monometallic Fe and Cu catalysts suffered major leaching, with Fe almost disappearing from the catalyst surface and Cu decreasing from ~5% to ~3%. On the contrary, the bimetallic catalysts showed good stability, related to low

metal leaching level. Rietvel refinement (Figure S9) also confirmed the loss of Cu from the Cu/ZrO_2 spent catalyst, while metal sintering was excluded due to the unchanged in Pd and Cu peaks shape/intensities. Therefore, the deactivation of the monometallic catalysts shown in Figure 4 can be prevalently ascribed to metal leaching under the studied conditions. Further studies are required to evaluate the long-term stability of the proposed catalysts.

CONCLUSIONS

The aim of this study was to investigate the effect of adding Pd as promoter to non-noble metals such as iron and copper for the hydrogenation of the aldehyde group of different model compounds representative of pyrolysis bio-oils. Therefore, Cu, Fe, Pd, PdCu, and PdFe supported on ZrO_2 were prepared by a wetness impregnation technique, characterised by different techniques and used in hydrogenation experiments. For furfural and vanillin, a 99% selectivity was obtained for mono-alcohols (FA and VA). The bi-metallic PdFe and PdCu displayed enhanced catalytic performance in terms of reactant conversion towards VA and FA and to a less extent sorbitol, compared to the monometallic catalysts. A better dispersion of the metals for the bimetallic catalysts compared to the monometallic ones, as was illustrated using STEM-EDX, is probably the main reason behind the higher conversion of the bimetallic catalysts. Interaction of the well dispersed Pd with Cu and Fe in the bimetallic catalysts was linked to their superior performance, due to their favourable H_2 adsorption at low temperature. This work shows that supported non-noble metal based catalyst containing Fe and Cu have high potential for the partial hydrogenation (or stabilisation) of bio-oil model compounds by promotion with (1 wt%) of Pd. Studies on the hydrogenation of lignocellulosic biomass derived bio oils with the catalysts reported here and their stability are in progress and will be reported in due course.

ASSOCIATED CONTENT

Supporting information

The Supporting Information is available free of charge on the ACS Publications website at DOI:

Experimental details on catalysts characterisation, Results for catalysts characterisation, surface analysis, TEM, XRD, H_2-TPR, NH_3-TPD, XPS, FTIR, Rietverd refinement of bare and spent catalysts, Selectivity for HDO of glucose, External and internal mass transfer limitations assessment. Pseudo first order reaction model of reactants conversion data.

AUTHOR INFORMATION

Corresponding author

*E-mail: A.Sanna@hw.ac.uk Tel.: +44(0)1314518108

ORCID

Giuseppe Bagnato 0000-0002-6576-9625

Gert H. ten Brink 0000-0002-7807-8831

Hero Jan Heeres 0000-0002-1249-543X

Bart J. Kooi 0000-0002-0311-4105

Federica Menegazzo 0000-0001-8023-6379

Cristina Pizzolitto 0000-0002-8268-4682

Aimaro Sanna 0000-0002-0816-489X

Michela Signoretto 0000-0002-0051-2968

Notes

The authors declare no competing financial interest.

AKNOLEDGEMENTS

The authors are grateful to Erasmus plus training program. Also, the authors thank M. B. Figueirêdo, L. Rohrbach and Dr. Z. Tang, Department of Chemical Engineering, Engineering, University of Groningen, for technical support and TEM analysis.

SYNOPSIS

The hydrogenation reaction of bio oil model compounds was studied in presence of bimetallic catalysts, producing promising results for industrial application.

REFERENCES

(1) Bagnato, G.; Sanna, A. Process and Techno-Economic Analysis for Fuel and Chemical Production by Hydrodeoxygenation of Bio-Oil. *Catalysts* **2019,** *9* (12), DOI: 10.3390/catal9121021.
(2) Bagnato, G.; Boulet, F.; Sanna, A. Effect of Li-LSX zeolite, NiCe/Al_2O_3 and NiCe/ZrO_2 on the production of drop-in bio-fuels by pyrolysis and hydrotreating of Nannochloropsis and isochrysis microalgae. *Energy* **2019,** *179*, 199-213, DOI: https://doi.org/10.1016/j.energy.2019.04.204.
(3) BioLiquids, B. https://www.btg-btl.com/en/applications/oilproperties.
(4) Menegazzo, F.; Ghedini, E.; Signoretto, M. 5-Hydroxymethylfurfural (HMF) Production from Real Biomasses. *Molecules* **2018,** *23* (9), 2201, DOI: 10.3390/molecules23092201
(5) Sanna, A.; Vispute, T. P.; Huber, G. W. Hydrodeoxygenation of the aqueous fraction of bio-oil with Ru/C and Pt/C catalysts. *Applied Catalysis B: Environmental* **2015,** *165*, 446-456, DOI: https://doi.org/10.1016/j.apcatb.2014.10.013.
(6) Giuliano, A.; Poletto, M.; Barletta, D. Pure hydrogen co-production by membrane technology in an IGCC power plant with carbon capture. *International Journal of Hydrogen Energy* **2018,** *43* (41), 19279-19292, DOI: https://doi.org/10.1016/j.ijhydene.2018.08.112.
(7) Diebold, J. P. *A review of the chemical and physical mechanisms of the storage stability of fast pyrolysis bio-oils*; NREL/SR-570-27613; TRN: AH200011%%11 United States 10.2172/753818 TRN: AH200011%%11 NREL English; ; National Renewable Energy Lab., Golden, CO (US): 1999; p Medium: ED; Size: vp., https://www.nrel.gov/docs/fy00osti/27613.pdf
(8) Liu, X.; Zhang, B.; Fei, B.; Chen, X.; Zhang, J.; Mu, X. Tunable and selective hydrogenation of furfural to furfuryl alcohol and cyclopentanone over Pt supported on biomass-derived porous heteroatom doped carbon. *Faraday Discussions* **2017,** *202* (0), 79-98, DOI: 10.1039/C7FD00041C.
(9) Bagnato, G.; Figoli, A.; Ursino, C.; Galiano, F.; Sanna, A. A novel Ru–polyethersulfone (PES) catalytic membrane for highly efficient and selective hydrogenation of furfural to furfuryl alcohol. *Journal of Materials Chemistry A* **2018,** *6* (12), 4955-4965, DOI: 10.1039/C7TA10575D.
(10) Li, X.; Jia, P.; Wang, T. Furfural: A Promising Platform Compound for Sustainable Production of C4 and C5 Chemicals. *ACS Catalysis* **2016,** *6* (11), 7621-7640, DOI: 10.1021/acscatal.6b01838.

(11) Fache, M.; Boutevin, B.; Caillol, S. Vanillin Production from Lignin and Its Use as a Renewable Chemical. *ACS Sustainable Chemistry & Engineering* **2016,** *4* (1), 35-46, DOI: 10.1021/acssuschemeng.5b01344.
(12) Metin, Ö.; Mendoza-Garcia, A.; Dalmızrak, D.; Gültekin, M. S.; Sun, S. FePd alloy nanoparticles assembled on reduced graphene oxide as a catalyst for selective transfer hydrogenation of nitroarenes to anilines using ammonia borane as a hydrogen source. *Catalysis Science & Technology* **2016,** *6* (15), 6137-6143, DOI: 10.1039/C6CY00118A.
(13) Lange, J.-P.; van der Heide, E.; van Buijtenen, J.; Price, R. Furfural—A Promising Platform for Lignocellulosic Biofuels. *ChemSusChem* **2012,** *5* (1), 150-166, DOI: doi:10.1002/cssc.201100648.
(14) Fulajtárova, K.; Soták, T.; Hronec, M.; Vávra, I.; Dobročka, E.; Omastová, M. Aqueous phase hydrogenation of furfural to furfuryl alcohol over Pd–Cu catalysts. *Applied Catalysis A: General* **2015,** *502*, 78-85, DOI: https://doi.org/10.1016/j.apcata.2015.05.031.
(15) Du, J.; Zhang, J.; Sun, Y.; Jia, W.; Si, Z.; Gao, H.; Tang, X.; Zeng, X.; Lei, T.; Liu, S.; Lin, L. Catalytic transfer hydrogenation of biomass-derived furfural to furfuryl alcohol over in-situ prepared nano Cu-Pd/C catalyst using formic acid as hydrogen source. *Journal of Catalysis* **2018,** *368*, 69-78, DOI: https://doi.org/10.1016/j.jcat.2018.09.025.
(16) Liu, L.; Lou, H.; Chen, M. Selective hydrogenation of furfural to tetrahydrofurfuryl alcohol over Ni/CNTs and bimetallic CuNi/CNTs catalysts. *International Journal of Hydrogen Energy* **2016,** *41* (33), 14721-14731, DOI: https://doi.org/10.1016/j.ijhydene.2016.05.188.
(17) Chen, B.; Li, F.; Huang, Z.; Yuan, G. Tuning catalytic selectivity of liquid-phase hydrogenation of furfural via synergistic effects of supported bimetallic catalysts. *Applied Catalysis A: General* **2015,** *500*, 23-29, DOI: https://doi.org/10.1016/j.apcata.2015.05.006.
(18) Sitthisa, S.; An, W.; Resasco, D. E. Selective conversion of furfural to methylfuran over silica-supported NiFe bimetallic catalysts. *Journal of Catalysis* **2011,** *284* (1), 90-101, DOI: https://doi.org/10.1016/j.jcat.2011.09.005.
(19) Sitthisa, S.; Pham, T.; Prasomsri, T.; Sooknoi, T.; Mallinson, R. G.; Resasco, D. E. Conversion of furfural and 2-methylpentanal on Pd/SiO2 and Pd–Cu/SiO2 catalysts. *Journal of Catalysis* **2011,** *280* (1), 17-27, DOI: https://doi.org/10.1016/j.jcat.2011.02.006.
(20) Shi, D.; Yang, Q.; Peterson, C.; Lamic-Humblot, A.-F.; Girardon, J.-S.; Griboval-Constant, A.; Stievano, L.; Sougrati, M. T.; Briois, V.; Bagot, P. A. J.; Wojcieszak, R.; Paul, S.; Marceau, E. Bimetallic Fe-Ni/SiO2 catalysts for furfural hydrogenation: Identification of the interplay between Fe and Ni during deposition-precipitation and thermal treatments. *Catalysis Today* **2019,** *334*, 162-172, DOI: https://doi.org/10.1016/j.cattod.2018.11.041.
(21) Shit, S. C.; Singuru, R.; Pollastri, S.; Joseph, B.; Rao, B. S.; Lingaiah, N.; Mondal, J. Cu–Pd bimetallic nanoalloy anchored on a N-rich porous organic polymer for high-performance hydrodeoxygenation of biomass-derived vanillin. *Catalysis Science & Technology* **2018,** *8* (8), 2195-2210, DOI: 10.1039/C8CY00325D.
(22) Zhang, F.; Zheng, S.; Xiao, Q.; Zhong, Y.; Zhu, W.; Lin, A.; Samy El-Shall, M. Synergetic catalysis of palladium nanoparticles encaged within amine-functionalized UiO-66 in the hydrodeoxygenation of vanillin in water. *Green Chemistry* **2016,** *18* (9), 2900-2908, DOI: 10.1039/C5GC02615F.
(23) Jiang, H.; Yu, X.; Peng, X.; Zhang, H.; Nie, R.; Lu, X.; Zhou, D.; Xia, Q. Efficient aqueous hydrodeoxygenation of vanillin over a mesoporous carbon nitride-modified Pd nanocatalyst. *RSC Advances* **2016,** *6* (73), 69045-69051, DOI: 10.1039/C6RA11851H.
(24) Santos, J. L.; Alda-Onggar, M.; Fedorov, V.; Peurla, M.; Eränen, K.; Mäki-Arvela, P.; Centeno, M. Á.; Murzin, D. Y. Hydrodeoxygenation of vanillin over carbon supported metal catalysts. *Applied Catalysis A: General* **2018,** *561*, 137-149, DOI: https://doi.org/10.1016/j.apcata.2018.05.010.
(25) Lazaridis, P. A.; Karakoulia, S.; Delimitis, A.; Coman, S. M.; Parvulescu, V. I.; Triantafyllidis, K. S. d-Glucose hydrogenation/hydrogenolysis reactions on noble metal (Ru, Pt)/activated carbon supported catalysts. *Catalysis Today* **2015,** *257*, 281-290, DOI: https://doi.org/10.1016/j.cattod.2014.12.006.
(26) Liu, J.; Zhang, L. L.; Zhang, J.; Liu, T.; Zhao, X. S. Bimetallic ruthenium–copper nanoparticles embedded in mesoporous carbon as an effective hydrogenation catalyst. *Nanoscale* **2013,** *5* (22), 11044-11050, DOI: 10.1039/C3NR03813K.

(27) Ro, I.; Aragao, I. B.; Brentzel, Z. J.; Liu, Y.; Rivera-Dones, K. R.; Ball, M. R.; Zanchet, D.; Huber, G. W.; Dumesic, J. A. Intrinsic activity of interfacial sites for Pt-Fe and Pt-Mo catalysts in the hydrogenation of carbonyl groups. *Applied Catalysis B: Environmental* **2018,** *231*, 182-190, DOI: https://doi.org/10.1016/j.apcatb.2018.02.058.
(28) Ftouni, J.; Muñoz-Murillo, A.; Goryachev, A.; Hofmann, J. P.; Hensen, E. J. M.; Lu, L.; Kiely, C. J.; Bruijnincx, P. C. A.; Weckhuysen, B. M. ZrO2 Is Preferred over TiO2 as Support for the Ru-Catalyzed Hydrogenation of Levulinic Acid to γ-Valerolactone. *ACS Catalysis* **2016,** *6* (8), 5462-5472, DOI: 10.1021/acscatal.6b00730.
(29) Gong, W.; Chen, C.; Zhang, Y.; Zhou, H.; Wang, H.; Zhang, H.; Zhang, Y.; Wang, G.; Zhao, H. Efficient Synthesis of Furfuryl Alcohol from H2-Hydrogenation/Transfer Hydrogenation of Furfural Using Sulfonate Group Modified Cu Catalyst. *ACS Sustainable Chemistry & Engineering* **2017,** *5* (3), 2172-2180, DOI: 10.1021/acssuschemeng.6b02343.
(30) Menegazzo, F.; Pizzolitto, C.; Zanardo, D.; Signoretto, M.; Buysschaert, C.; Bény, G.; Di Michele, A. Hydrogen Production by Ethanol Steam Reforming on Ni-Based Catalysts: Effect of the Support and of CaO and Au Doping. *ChemistrySelect* **2017,** *2* (29), 9523-9531, DOI: 10.1002/slct.201702053.
(31) Pinna, F.; Selva, M.; Signoretto, M.; Strukul, G.; Boccuzzi, F.; Benedetti, A.; Canton, P.; Fagherazzi, G. Pd-Fe/SiO2 Catalysts in the Hydrogenation of 2,4-Dinitrotoluene. *Journal of Catalysis* **1994,** *150* (2), 356-367, DOI: https://doi.org/10.1006/jcat.1994.1354.
(32) Boot, L. A.; van Dillen, A. J.; Geus, J. W.; van Buren, F. R. Iron-Based Dehydrogenation Catalysts Supported on Zirconia. I. Preparation and Characterization. *Journal of Catalysis* **1996,** *163* (1), 186-194, DOI: https://doi.org/10.1006/jcat.1996.0318.
(33) Guglielminotti, E. Spectroscopic Characterization of the Fe/ZrO2 System: 1. CO Adsorption. *The Journal of Physical Chemistry* **1994,** *98* (18), 4884-4891, DOI: 10.1021/j100069a019.
(34) Crystallography Open Database, http://www.crystallography.net/cod/.
(35) Sato, A. G.; Volanti, D. P.; Meira, D. M.; Damyanova, S.; Longo, E.; Bueno, J. M. C. Effect of the ZrO2 phase on the structure and behavior of supported Cu catalysts for ethanol conversion. *Journal of Catalysis* **2013,** *307*, 1-17, DOI: https://doi.org/10.1016/j.jcat.2013.06.022.
(36) Rhodes, M. D.; Pokrovski, K. A.; Bell, A. T. The effects of zirconia morphology on methanol synthesis from CO and H2 over Cu/ZrO2 catalysts: Part II. Transient-response infrared studies. *Journal of Catalysis* **2005,** *233* (1), 210-220, DOI: https://doi.org/10.1016/j.jcat.2005.04.027.
(37) Azenha, C. S. R.; Mateos-Pedrero, C.; Queirós, S.; Concepción, P.; Mendes, A. Innovative ZrO2-supported CuPd catalysts for the selective production of hydrogen from methanol steam reforming. *Applied Catalysis B: Environmental* **2017,** *203*, 400-407, DOI: https://doi.org/10.1016/j.apcatb.2016.10.041.
(38) Agostini, G.; Groppo, E.; Piovano, A.; Pellegrini, R.; Leofanti, G.; Lamberti, C. Preparation of Supported Pd Catalysts: From the Pd Precursor Solution to the Deposited Pd2+ Phase. *Langmuir* **2010,** *26* (13), 11204-11211, DOI: 10.1021/la1005117.
(39) Vedyagin, A. A.; Volodin, A. M.; Kenzhin, R. M.; Chesnokov, V. V.; Mishakov, I. V. CO Oxidation over Pd/ZrO2 Catalysts: Role of Support's Donor Sites. *Molecules* **2016,** *21* (10), 1289, DOI: 10.3390/molecules21101289
(40) Qi, B.; Di, L.; Xu, W.; Zhang, X. Dry plasma reduction to prepare a high performance Pd/C catalyst at atmospheric pressure for CO oxidation. *Journal of Materials Chemistry A* **2014,** *2* (30), 11885-11890, DOI: 10.1039/C4TA02155J.
(41) Jin, J.; Li, C.; Tsang, C.-W.; Xu, B.; Liang, C. Catalytic combustion of methane over Pd/Ce–Zr oxides washcoated monolithic catalysts under oxygen lean conditions. *RSC Advances* **2015,** *5* (124), 102147-102156, DOI: 10.1039/C5RA13223A.
(42) Wang, Y. H.; Gao, W. G.; Wang, H.; Zheng, Y. E.; Na, W.; Li, K. Z. Structure–activity relationships of Cu–ZrO2 catalysts for CO2 hydrogenation to methanol: interaction effects and reaction mechanism. *RSC Advances* **2017,** *7* (14), 8709-8717, DOI: 10.1039/C6RA28305E.
(43) Wang, G.; Chen, L.; Sun, Y.; Wu, J.; Fu, M.; Ye, D. Carbon dioxide hydrogenation to methanol over Cu/ZrO2/CNTs: effect of carbon surface chemistry. *RSC Advances* **2015,** *5* (56), 45320-45330, DOI: 10.1039/C5RA04774A.

(44) Li, K.; Wang, H.; Wei, Y.; Yan, D. Direct conversion of methane to synthesis gas using lattice oxygen of CeO2–Fe2O3 complex oxides. *Chemical Engineering Journal* **2010,** *156* (3), 512-518, DOI: https://doi.org/10.1016/j.cej.2009.04.038.
(45) Albuquerque, E. M.; Borges, L. E. P.; Fraga, M. A.; Sievers, C. Relationship between Acid–Base Properties and the Activity of ZrO2-Based Catalysts for the Cannizzaro Reaction of Pyruvaldehyde to Lactic Acid. *ChemCatChem* **2017,** *9* (14), 2675-2683, DOI: 10.1002/cctc.201700305.
(46) Jiang, X.; Koizumi, N.; Guo, X.; Song, C. Bimetallic Pd–Cu catalysts for selective CO2 hydrogenation to methanol. *Applied Catalysis B: Environmental* **2015,** *170-171*, 173-185, DOI: https://doi.org/10.1016/j.apcatb.2015.01.010.
(47) Nie, X.; Jiang, X.; Wang, H.; Luo, W.; Janik, M. J.; Chen, Y.; Guo, X.; Song, C. Mechanistic Understanding of Alloy Effect and Water Promotion for Pd-Cu Bimetallic Catalysts in CO2 Hydrogenation to Methanol. *ACS Catalysis* **2018,** *8* (6), 4873-4892, DOI: 10.1021/acscatal.7b04150.
(48) Sitthisa, S.; Sooknoi, T.; Ma, Y.; Balbuena, P. B.; Resasco, D. E. Kinetics and mechanism of hydrogenation of furfural on Cu/SiO2 catalysts. *Journal of Catalysis* **2011,** *277* (1), 1-13, DOI: https://doi.org/10.1016/j.jcat.2010.10.005.
(49) Di, L. B.; Duan, D. Z.; Park, D. W.; Ahn, W. S.; Lee, B. J.; Zhang, X. L. Cold Plasma for Synthesizing High Performance Bimetallic PdCu catalysts: Effect of Reduction Sequence and Pd/Cu Atomic Ratios. *Topics in Catalysis* **2017,** *60* (12), 925-933, DOI: 10.1007/s11244-017-0757-5.
(50) Hong, Y.; Zhang, H.; Sun, J.; Ayman, K. M.; Hensley, A. J. R.; Gu, M.; Engelhard, M. H.; McEwen, J.-S.; Wang, Y. Synergistic Catalysis between Pd and Fe in Gas Phase Hydrodeoxygenation of m-Cresol. *ACS Catalysis* **2014,** *4* (10), 3335-3345, DOI: 10.1021/cs500578g.
(51) Rezaei, P. S.; Shafaghat, H.; Daud, W. M. A. W. Aromatic hydrocarbon production by catalytic pyrolysis of palm kernel shell waste using a bifunctional Fe/HBeta catalyst: effect of lignin-derived phenolics on zeolite deactivation. *Green Chemistry* **2016,** *18* (6), 1684-1693, DOI: 10.1039/C5GC01935D.
(52) Singh, H.; Rai, A.; Yadav, R.; Sinha, A. K. Glucose hydrogenation to sorbitol over unsupported mesoporous Ni/NiO catalyst. *Molecular Catalysis* **2018,** *451*, 186-191, DOI: https://doi.org/10.1016/j.mcat.2018.01.010.
(53) Romero, A.; Nieto-Márquez, A.; Alonso, E. Bimetallic Ru:Ni/MCM-48 catalysts for the effective hydrogenation of d-glucose into sorbitol. *Applied Catalysis A: General* **2017,** *529*, 49-59, DOI: https://doi.org/10.1016/j.apcata.2016.10.018.
(54) Li, N.; Huber, G. W. Aqueous-phase hydrodeoxygenation of sorbitol with Pt/SiO2–Al2O3: Identification of reaction intermediates. *Journal of Catalysis* **2010,** *270* (1), 48-59, DOI: https://doi.org/10.1016/j.jcat.2009.12.006.
(55) Zhang, X.; Durndell, L. J.; Isaacs, M. A.; Parlett, C. M. A.; Lee, A. F.; Wilson, K. Platinum-Catalyzed Aqueous-Phase Hydrogenation of d-Glucose to d-Sorbitol. *ACS Catalysis* **2016,** *6* (11), 7409-7417, DOI: 10.1021/acscatal.6b02369.
(56) Zanuttini, M. S.; Gross, M.; Marchetti, G.; Querini, C. Furfural hydrodeoxygenation on iron and platinum catalysts. *Applied Catalysis A: General* **2019,** *587*, 117217, DOI: https://doi.org/10.1016/j.apcata.2019.117217.
(57) Zhang, H.; Shao, S.; Xiao, R.; Shen, D.; Zeng, J. Characterization of Coke Deposition in the Catalytic Fast Pyrolysis of Biomass Derivates. *Energy & Fuels* **2014,** *28* (1), 52-57, DOI: 10.1021/ef401458y.
(58) Sandford, S. A.; Bernstein, M. P.; Materese, C. K. The infrared spectra of polycyclic aromatic hydrocarbons with excess peripheral H atoms (Hn -PAHs) and their relation to the 3.4 and 6.9 μm PAH emission features. *The Astrophysical Journal Supplement Series* **2013,** *205* (1), 8, DOI: 10.1088/0067-0049/205/1/8.

For Table of Contents Use Only